

Variable-angle sample-spinning high resolution NMR of solids^{a)}

Subramanian Ganapathy, Suzanne Schramm, and Eric Oldfield^{b)}

School of Chemical Sciences, University of Illinois at Urbana, Urbana, Illinois 61801
(Received 8 June 1982; accepted 14 July 1982)

We have obtained high-resolution solid-state NMR spectra of a variety of nonintegral-spin quadrupolar nuclei (²³Na, ⁵¹V, and ⁵⁵Mn) under conditions of "magic-angle" sample-spinning (MASS) and "variable-angle" sample-spinning (VASS). We show for systems in which the second-order quadrupole interaction dominates the breadth of the (1/2, -1/2) spin transition, that optimum line narrowing is achieved by rapid sample rotation at angles other than the familiar $\theta = 54.7^\circ$ "magic-angle." The effect originates in the more complex angle dependence of the second-order quadrupole interaction, rather than the more familiar $P_2(\cos \theta)$ dependence of dipolar and chemical shift interactions, and theoretical VASS line shapes for a variety of spinning angles, and electric field gradient tensor asymmetry parameters (η), are presented. We show that VASS NMR at low fields generates complex spectral line shapes, which at some angles exhibit well-resolved centerbands and spinning sidebands. We also discuss briefly, with examples, the complexities introduced by the presence of dipolar and/or chemical shift anisotropy interactions in such experiments and investigate the question of the optimum field-strengths for NMR of quadrupolar nuclei. Our results indicate that the VASS NMR technique appears to have considerable utility in obtaining high-resolution NMR spectra of a wide variety of quadrupolar nuclei in inorganic solids, especially those with relatively small ($\lesssim 5$ MHz) quadrupole coupling constants.

I. INTRODUCTION

Conventional "magic-angle" sample spinning (MASS), introduced by Andrew and co-workers^{1,2} and by Lowe,³ has been in existence for almost a quarter of a century, and there have been numerous applications of the technique to high-resolution NMR of spin- $\frac{1}{2}$ nuclei in solids.⁴ There has, however, been a rather surprising paucity of data on the application of the MASS technique to the study of nuclei having spins $I > 1$. Early investigators showed that the MASS technique could be usefully applied to nuclei having small quadrupole coupling constants, e.g., ²⁷Al in AlP⁵ or ¹³³Cs in CsCl,⁶ and more recently, the technique has been applied to the ²H nucleus, where e^2qQ/h values are also rather small ($\lesssim 200$ kHz), and a combination of synchronous sampling and other specialized techniques has yielded high-resolution ²H spectra, by averaging of the (first-order) quadrupole interaction.⁷

Most nuclei in the Periodic Table, however, have e^2qQ/h values considerably in excess of the 200 kHz displayed by deuterium, and such MASS experiments are not feasible, since the residual breadths, due to rotor instability, are $\sim 2.5\%$ per degree deviation, at the "magic-angle." Thus, a 1 degree rotor oscillation yields a ~ 25 kHz residual breadth for a system having $e^2qQ/h = 1$ MHz. Fortunately, however, most of these same nuclei in the Periodic Table possess *nonintegral* spins $I = 3/2, 5/2, 7/2$, and $9/2$. There is thus a central ($\frac{1}{2}, -\frac{1}{2}$) transition, which to first order is not broadened

by quadrupole effects,⁸ and this transition has recently been the subject of considerable interest⁹⁻¹⁵ as a means of obtaining high-resolution NMR in inorganic solids, especially those systems of importance as industrial catalysts.

In this article we discuss our recent progress in NMR of quadrupolar nuclei in inorganic solids, considering in particular the optimum experimental conditions for obtaining high-resolution. Most importantly, we find for systems with large e^2qQ/h values (of the order of a few MHz) that spinning angles other than the familiar 54.7° are most efficient in line narrowing. For example, for ²³Na in Na₂MoO₄, an order-of-magnitude reduction in breadth of the central transition is achieved by rapid rotation at $\beta = 36^\circ$ or 75° , over twice that achieved at 54.7° . We thus present in this paper both experimental results, and theoretical calculations, of NMR line shapes under conditions of rapid "variable-angle" sample rotation, and we also discuss the importance of other factors, such as field-strength optimization, and the presence of dipolar and chemical shift interactions, on the experimental spectra. Overall, our data clearly indicate that VASS is a promising new approach for obtaining high-resolution spectra of quadrupolar nuclei in inorganic solids.

II. THEORY FOR VASS LINE SHAPES

We consider a quadrupolar nucleus having a nonintegral spin, and confine ourselves to the central ($\frac{1}{2}, -\frac{1}{2}$) spin transition. Neglecting anisotropic chemical shifts, the total Hamiltonian in the high field regime ($|H_z| \gg |H_Q|$) for the static case may be written as

$$\mathcal{H} = \mathcal{H}_z + \mathcal{H}_Q, \quad (1)$$

where the Zeeman Hamiltonian is

$$\mathcal{H}_z = -\gamma \hbar H_0 I_z, \quad (2)$$

and the nuclear quadrupolar Hamiltonian, treated as a

^{a)} Part of this work was supported by the US National Institutes of Health (grants CA-00595, HL-19481), by the US National Science Foundation (grants PCM 79-23170, 81-17813), and by the American Heart Association (grant 80-867), and has benefitted from the use of facilities made available through the University of Illinois NSF Regional Instrumentation Facility (grant CHE 79-16100).

^{b)} USPHS Research Career Development Awardee, 1979-1984.

perturbation, is

$$\mathcal{H}_Q = \frac{e^2 q Q}{4I(2I-1)} [3I_x^2 - I^2 + \eta(I_x^2 - I_y^2)], \quad (3)$$

where the symbols have their usual meanings,⁸ and the spin operators of \mathcal{H}_Q are evaluated in a coordinate system in which the field gradient tensor is diagonal.

For a polycrystalline sample spun at an angle β with respect to the static magnetic field H_0 with an angular velocity ω_r , the Hamiltonian, \mathcal{H} , becomes time-dependent. However, the variation is slow since ω_r is several orders of magnitude smaller than the perturbing frequency ($\nu_r = \omega_r/2\pi \approx 2-6$ kHz; $e^2 q Q/h \approx 1-5$ MHz). The Hamiltonian is quasistationary, and as in the adiabatic approximation we may use the instantaneous eigenvalues of \mathcal{H} , allowing us to calculate the energy of the NMR resonance at a certain molecular orientation at time "t" as follows:

$$\mathcal{H}(t)\psi(t) = E(t)\psi(t). \quad (4)$$

As pointed out by Haeberlen,¹⁶ considerations as to whether the spin magnetization can follow adiabatically the motion of the sample will be required only in the weak-field case. For our high-field case, the approximation is thus valid.

For the most general case of $\eta \neq 0$, we thus transform the spin operators of Eq. (3) from the principal axis system (PAS; x', y', z') of the quadrupole tensor, to the Zeeman axis system (ZAS; x, y, z), via the rotation axis system (RAS). Details of this transformation

procedure are given in detail by Naito *et al.*¹⁷ The elements of the coordinate transformation matrix are trigonometric functions of the Euler angles of the RAS¹⁸: $\beta'(0$ to $\pi)$, $\phi(0$ to $2\pi)$ and $\psi(0$ to $2\pi)$, and the angle β between the spinning axis and the static magnetic field H_0 . Due to spinning at a frequency $\nu_r = \omega_r/2\pi$, ψ is time dependent, and is given by $\psi = \omega_r t + \psi_0$, where ψ_0 is the initial angle at $t=0$. We use the Zeeman quantized spin functions $|m_i\rangle$ as the basis set, and calculate the matrix elements of $\mathcal{H}_Q(t)$. Treating $\mathcal{H}_Q(t)$ as a perturbation on \mathcal{H}_Z , the transition energy for the central transition ($\frac{1}{2}, -\frac{1}{2}$) of a nonintegral spin I ($I > 1$) at a given molecular orientation at time "t" is calculated using second-order perturbation theory as follows:

$$\Delta E_{\beta,\phi,\psi}(t) = E_{-1/2}^{(2)}(t) - E_{1/2}^{(2)}(t),$$

$$\nu = \nu_L + \left[\frac{3e^2 q Q}{2I(2I-1)h} \right]^2 \left[\frac{I(I+1) - 3/4}{9\nu_L} \right] [X - 2Y], \quad (5)$$

where

$$X = \frac{1}{16} \{ [3(A_{31}^2 - A_{32}^2) + \eta(A_{11}^2 + A_{22}^2 - A_{21}^2 - A_{12}^2)]^2$$

$$+ 4[(3A_{31}A_{32} + \eta(A_{11}A_{12} - A_{21}A_{22}))^2] \},$$

$$Y = \frac{1}{4} \{ [3A_{33}A_{31} + \eta(A_{13}A_{11} - A_{23}A_{21})]^2$$

$$+ [3A_{33}A_{33} + \eta(A_{12}A_{13} - A_{22}A_{23})]^2 \},$$

and ν_L is the nuclear Larmor frequency. The A_{ij} s are the matrix elements of A , where $A = BC$. Here, B represents the first transformation from PAS to RAS, and C the transformation from RAS to ZAS. These have the explicit forms

$$B = \begin{bmatrix} \cos \psi \cos \phi - \cos \beta' \sin \phi \sin \psi & -\sin \psi \cos \phi - \cos \beta' \sin \phi \cos \psi & \sin \beta' \sin \phi \\ \cos \psi \sin \phi + \cos \beta' \cos \phi \sin \psi & -\sin \psi \sin \phi + \cos \beta' \cos \phi \cos \psi & -\sin \beta' \cos \phi \\ \sin \psi \sin \beta' & \cos \psi \sin \beta' & \cos \beta' \end{bmatrix}, \quad (7)$$

$$C = \begin{bmatrix} 1 & 0 & 0 \\ 0 & \cos \beta & -\sin \beta \\ 0 & \sin \beta & \cos \beta \end{bmatrix}. \quad (8)$$

For rapid sample spinning, such that ν_r is greater than the second-order quadrupole linebreadth of the ($\frac{1}{2}, -\frac{1}{2}$) transition, $\Delta E(t)$ may be averaged over one cycle to give

$$\overline{\Delta E_{\beta,\phi,\psi}}(t) = \frac{1}{2\pi} \int_0^{2\pi} \Delta E_{\beta,\phi,\psi}(\psi) d\psi. \quad (9)$$

The actual line shape function $S(\nu)$ is a convolution of the rotation averaged powder shape, $\overline{\Delta E_{\beta,\phi,\psi}}(t)$, and a broadening function, taken as Gaussian for our case, $F[\nu - \overline{\Delta E_{\beta,\phi,\psi}}(t)]$.

In our calculations, the values of $\overline{\Delta E_{\beta,\phi,\psi}}(t)$ were evaluated numerically on a Control Data Corporation Cyber-175 computer system, using 5° increments for $\psi = \omega_r t + \psi_0$, in the range $0^\circ-360^\circ$, for a given molecular orientation (i.e., for fixed β' and ϕ values). The average $\overline{\Delta E_{\beta,\phi,\psi}}(t)$ was then calculated for each combination of β'

and ϕ , and the theoretically averaged line positions convoluted with a Gaussian broadening function to give the actual experimental line shape. Note that our expressions reduce to those of Baugher *et al.*¹⁹ for the static case ($\beta = 0$, $\phi = \phi$, $\psi = 0$, $\beta' = \theta$).

III. RESULTS AND DISCUSSION

We show in Fig. 1 theoretical variable-angle sample-spinning spectra for the central ($\frac{1}{2}, -\frac{1}{2}$) spin transition, under conditions of rapid sample-rotation, for asymmetry parameters (η) of 0 [Fig. 1(A)], 0.3 [Fig. 1(B)], 0.6 [Fig. 1(C)], and 1.0 [Fig. 1(D)]. Interestingly, the case of 90° sample-spinning ($\eta = 0$) was investigated in Andrew's original work¹ and Nolle has verified this early prediction experimentally.²⁰

The results of Fig. 1 clearly indicate that a wide variety of experimental line shapes may be generated using the VASS technique. In addition, it appears in all cases that more efficient line narrowing may be achieved by spinning at angles other than the conventional 54.7° "magic-angle." For example, even with

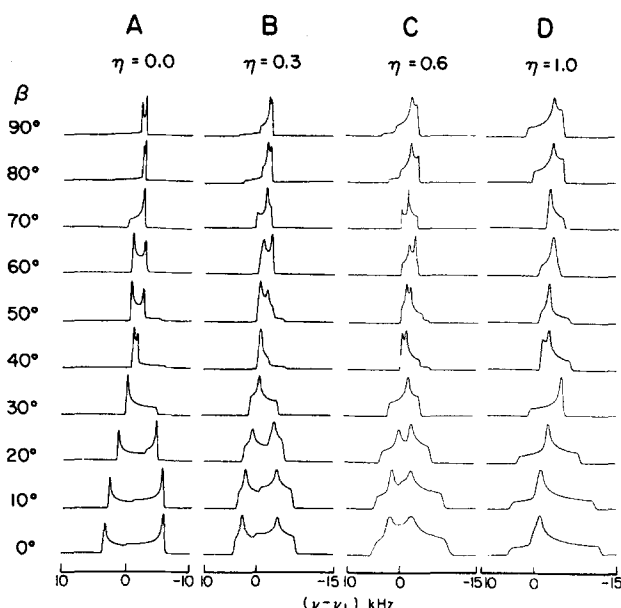


FIG. 1. Computer simulated variable-angle sample-spinning line shapes for the central ($\frac{1}{2}, -\frac{1}{2}$) transition of ^{23}Na ($I = 3/2$), broadened by second-order quadrupole effects, and under the condition of "rapid" sample rotation. The simulations are shown for different values of the rotation angle β in the range $0-90^\circ$, in 10° intervals, for $\eta = 0.0, 0.3, 0.6$, and 1.0 . The following parameters were used: $e^2qQ/h = 2.6$ MHz, $\nu_L = 95.25$ MHz, and 100 Hz Gaussian broadening. $(\nu - \nu_L)$ corresponds to the frequency deviation from the Larmor frequency, ν_L .

the coarse (10°) selection of spectra shown in Fig. 1(A), it seems most likely that spinning at $\beta \approx 30-40^\circ$ or $\beta \approx 80^\circ$ may be more effective than in the range $50-60^\circ$ (near the "magic-angle"), at least for $\eta = 0$.

We have therefore recorded experimental VASS spectra of the ^{23}Na nucleus in Na_2MoO_4 ($e^2qQ/h = 2.6$ MHz, $\eta = 0$, Ref. 21) and in Na_2SO_4 ($e^2qQ/h = 2.6$ MHz, $\eta = 0.6$, Ref. 22) at 1° increments in the range $0-90^\circ$ (data not shown) and at the "magic-angle" of 54.7° , and selected examples are given in Figs. 2 and 3.

We show in Fig. 2, A-D, 95.2 MHz sodium-23 Fourier transform NMR spectra of a ~ 400 mg sample of freshly dried Na_2MoO_4 , static, and spinning at ≈ 5 kHz, at the angles indicated. Also shown are spectral simulations obtained using the method described in Sec. II. The spectrum of the static sample is in good agreement with that calculated theoretically, and any differences presumably reside in a small orientation-dependent dipolar interaction, which was not included in the simulation. Upon spinning at the "magic-angle" of 54.7° , Fig. 2(B), there is an approximately fourfold decrease in linebreadth, in agreement with theory, and as observed by others.^{11,14} The additional features are due to spinning sidebands. Importantly, however, when spinning at $\beta = 36^\circ$ or at $\beta = 75^\circ$, even further line narrowing is observed experimentally, Figs. 2(C), 2(D) and these results are in excellent accord with those predicted on the basis of the theory discussed above, and the known electric quadrupole coupling constant and asymmetry parameter.²¹ Interestingly, our results in-

dicate considerably larger first-order spinning-sidebands when spinning at $\beta = 36^\circ$ than at $\beta = 75^\circ$, an effect that is accentuated at low field (see below), indicating the need for additional calculations of side band intensities. Notably, both the 36° and 75° VASS spectra show an approximately tenfold decrease in breadth over that of the static spectrum, an additional factor of 2 decrease in linewidth over that obtained using conventional MASS techniques.

The results of Fig. 3 were obtained on a sample of freshly dried Na_2SO_4 ($e^2qQ/h = 2.6$ MHz, $\eta = 0.6 \pm 0.1$, Ref. 22) at 95.2 MHz (corresponding to a magnetic field strength of 8.45 T) and show similar line narrowing to that seen with the zero asymmetry-parameter species Na_2MoO_4 Fig. 2. The static spectrum [Fig. 3(A)] is in good agreement with that expected on the basis of the theory outlined above, slight differences between the experimental and calculated line shapes again being due, presumably, to orientation-dependent dipolar broadening in the rigid lattice, which was not considered in the simulation.

On rapid "magic-angle" spinning ($\beta = 54.7^\circ$), there is

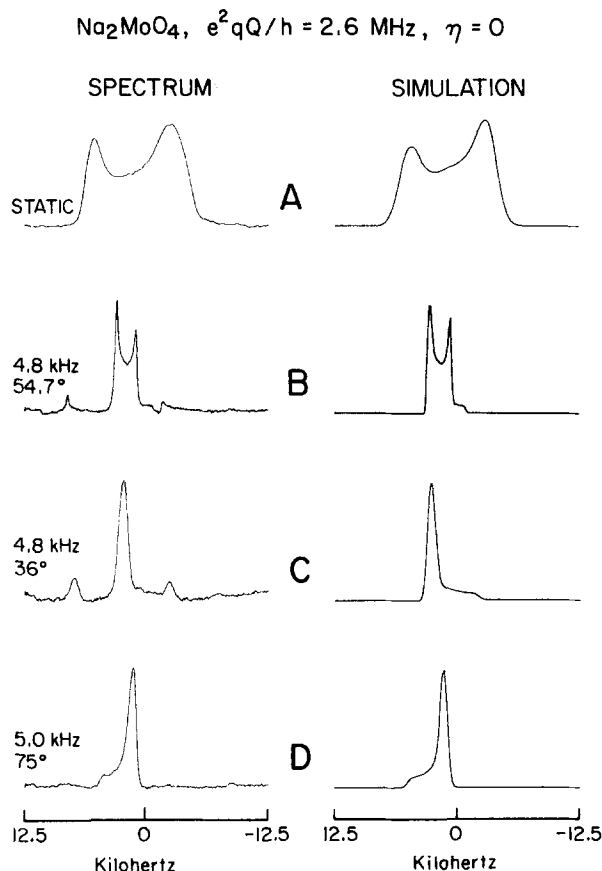


FIG. 2. 95.2 MHz ^{23}Na Fourier transform NMR spectra, and computer simulations, of the central ($\frac{1}{2}, -\frac{1}{2}$) transition of Na_2MoO_4 (corresponding to a magnetic field strength of 8.45 T). (A) Static spectrum; (B)-(D) spinning spectra corresponding to (B) $\beta = 54.7^\circ$; (C) $\beta = 36^\circ$; (D) $\beta = 75^\circ$. Spectra were obtained using spinning rates of ~ 5 kHz, 3 scans, recycle time = 20 s. Values of between 50 and 300 Hz broadening were used in the computer simulations.

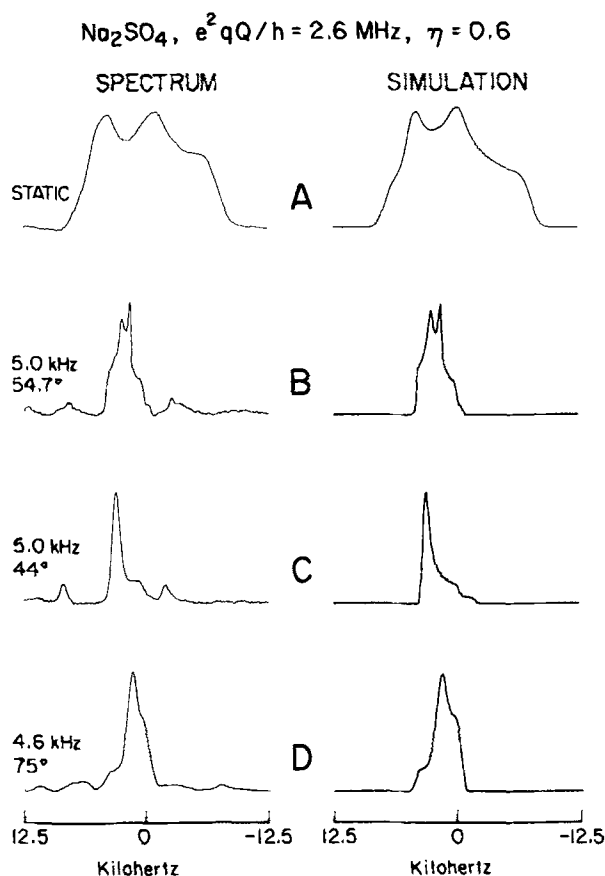


FIG. 3. 95.2 MHz ^{23}Na Fourier transform NMR spectra, and computer simulations, of the central $(\frac{1}{2}, -\frac{1}{2})$ transition of Na_2SO_4 . (A) Static spectrum; (B)–(D) spinning spectra corresponding to (B) $\beta = 54.7^\circ$; (C) $\beta = 44^\circ$; (D) $\beta = 75^\circ$. Spectra were obtained using spinning rates of $\sim 5 \text{ kHz}$, 120 scans, recycle time = 1.0 s. Values of between 50 and 100 Hz broadening were used in the computer simulations.

again an approximately fourfold reduction in the spectral breadth, Fig. 3(B), in good agreement with the results of Kundla *et al.*¹¹ on the ^{23}Na NMR spectrum of natrolite (a zeolite), where e^2qQ/h and η values of 1.76 MHz and 0.643 have been observed.²³ However, the observed ^{23}Na NMR spectrum displays a well-defined splitting which may be eliminated in the variable-angle spinning experiment by rapid rotation at $\beta = 44^\circ$, Fig. 3(C). This is the optimum theoretical angle for $\eta \sim 0.6$ (assuming only second-order quadrupolar broadening effects). Note that for this large asymmetry parameter, the optimum angle is some 6° larger than in the case of Na_2MoO_4 , where $\eta = 0$.

At much larger angles, there are still significant decreases in line width, but at 75° the overall linebreadth is approximately the same as that achieved with conventional MASS, [Figs. 3(B) and 3(D)]. Thus, the results of Figs. 2 and 3 indicate that the "optimum" angles for linenarrowing in the VASS NMR experiment are a strong function of the asymmetry parameter of the nucleus in question. The results of Figs. 1–3 do indicate, however, that rotation angles other than the familiar 54.7° , may often be appropriate for nuclei in which the second-order quadrupole interaction dominates. Note also, of

course, that for optimum-line narrowing, the rate of rotation ν_r should be in excess of the breadth of the static $(\frac{1}{2}, -\frac{1}{2})$ transition, when expressed in frequency units. The effects seen at lower spinning speeds are discussed briefly below in relation to the field-strength optimization of high-resolution NMR of quadrupolar solids.

IV. OTHER FACTORS INFLUENCING VASS OF QUADRUPOLEAR SOLIDS

In this final section we briefly discuss, with experimental examples, general considerations for high-resolution NMR of quadrupolar solids, especially with respect to field-strength/spinning-frequency optimization and the effects of other (dipolar and magnetic shift anisotropy) interactions on the VASS experiment.

We show in Fig. 4(A) static and spinning spectra of ^{23}Na in Na_2MoO_4 , at several different field strengths. At 3.52 T (corresponding to a ^{23}Na resonance of 39.7 MHz, or a ^1H resonance frequency of 150 MHz) the

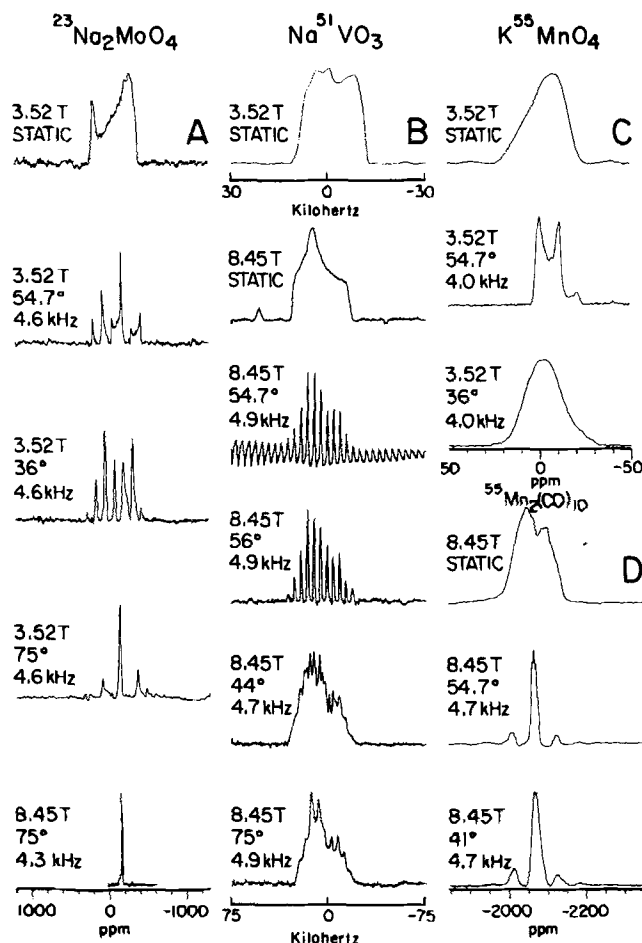


FIG. 4. Field and spinning-angle dependence of ^{23}Na , ^{51}V , and ^{55}Mn NMR spectra of several inorganic solids. (A) Sodium-23 NMR of Na_2MoO_4 ($e^2qQ/h = 2.6 \text{ MHz}$, $\eta = 0$) at 3.52 and 8.45 T. The spinning rate, angle, and field strength are indicated; (B) Vanadium-51 NMR of NaVO_3 ($e^2qQ/h \approx 3.6 \text{ MHz}$, $\eta = 0.6$) at 3.52 and 8.45 T. The spinning rate, angle, and field strength are indicated; (C) Manganese-55 NMR of KMnO_4 at 3.52 T. The spinning rate and angle are indicated; (D) Manganese-55 NMR of $\text{Mn}_2(\text{CO})_{10}$ at 8.45 T. The spinning rate and angle are indicated.

breadth of the $(\frac{1}{2}, -\frac{1}{2})$ central transition is some 20 kHz, and as expected spinning at the "magic-angle" of 54.7° at ~ 4.6 kHz produces a rather complex spectrum, since neither the angle nor rotation rate are optimal. By contrast, spinning at 36° produces a series of well resolved resonances, Fig. 4(A), but the spectrum is unnecessarily complex since there is in fact only a single sodium present, but some 5–6 sidebands are observed upon "slow" sample rotation. We have, however, found at $\beta = 75^\circ$, and the same rotation rate, that the *first-order sidebands are absent*, and that relatively high-resolution is achievable, even at low-field, Fig. 4(A). Higher frequency operation produces even smaller sidebands, since as indicated in Eq. 5, the breadth of the $(\frac{1}{2}, -\frac{1}{2})$ transition *decreases* linearly with magnetic field. For the ^{23}Na nucleus in question, the residual breadths at 8.45 T (360 MHz ^1H resonance frequency) and 11.7 T (500 MHz ^1H resonance frequency) are thus considerably narrower than those at lower field, being ~ 8 kHz at 8.5 T or only ~ 6 kHz at 11.7 T. Rapid (≈ 4 –5 kHz) sample rotation at these higher field strengths therefore gives considerably simpler spectra than those obtained at the lower (3.52 T) field values, as shown in Fig. 4(A). It should be borne in mind, however, that for systems having identical chemical shifts but different quadrupole coupling constants, low-field NMR operation may be preferable, since the differential quadrupolar lineshifts may be used as "spreading parameters." Such results have been observed in our laboratory using the ^{11}B nucleus in a borosilicate glass.²⁴

In the presence of a significant chemical shift anisotropy and a moderate quadrupole coupling constant, the situation is of course not so simple, as we have discussed elsewhere.¹³ By way of example, we show in Fig. 4(B) ^{51}V NMR spectra of NaVO_3 , static at 3.52 and 8.45 T, and spinning at 8.45 T.¹³ At low field the observed line-shape is complex, due to significant contributions from both CSA and second-order quadrupolar effects. At high field, however, there is an increase in relative contribution of the chemical shift anisotropy by a factor of $(360/150)^2$, or about 6. As a result, the CSA overwhelmingly dominates the observed spectrum, and conventional MASS is effective in producing numerous sidebands, both from the central (CSA) and (quadrupolar) satellite transitions. As pointed out elsewhere,¹³ but included here for completeness, we find by spinning $\sim 1^\circ$ off axis, near the "magic-angle," that the satellite absorption may be effectively removed, due to a large residual broadening. Also, as expected, we find that spinning at the optimum angles for reducing the second order quadrupole interaction ($\sim 44^\circ, 75^\circ; \eta = 0.6$, Ref. 19) produces rather uninformative line shapes, Fig. 4(B), at both 3.52 and 8.45 T. Only at much lower field strengths will the second order quadrupole interaction dominate the $(\frac{1}{2}, -\frac{1}{2})$ transition with NaVO_3 . Thus, for NaVO_3 (^{51}V , $I = 7/2$, $e^2qQ/h = 3.6$ MHz, $\eta = 0.6$; CSA $\sim -213, -56, 369$ ppm, Refs. 13, 19) high-field MASS appears the most appropriate technique to attempt to obtain high-resolution NMR spectral information. Note for nuclei having similar e^2qQ/h values but smaller spins, e.g., $I = 3/2$, that such a convenient elimination

of the second-order breadth would not be feasible.¹²

Finally, we show in Fig. 4(C) and 4(D) the effects of dipolar interactions in two experimental systems:

^{55}Mn in KMnO_4 , and in the metal-metal bond containing carbonyl, $\text{Mn}_2(\text{CO})_{10}$. Both we and Burton and Harris¹⁴ have recently obtained low-field MASS spectra of KMnO_4 in the solid state, Fig. 4(C). The ^{55}Mn NMR spectrum of static KMnO_4 [and $\text{Mn}_2(\text{CO})_{10}$] is an essentially featureless blob, due to the importance, we believe, of K-Mn and Mn-Mn dipole-dipole interactions, in addition to a small second-order quadrupole interaction ($e^2qQ/h = 1.6$ MHz, $\eta = 0$, Ref. 14). On conventional MASS the spectrum of KMnO_4 does, however, exhibit a well resolved line shape, characteristic of a second-order powder pattern of a nucleus having $\eta = 0$ under 54.7° MASS rotation, due to averaging of dipolar and second-order quadrupolar interactions. As discussed above, and as shown in Figs. 1 and 2 we might expect more efficient line narrowing, i.e., collapse of the "doublet" line shape of Fig. 4(C) by rapid sample-spinning at $\beta = 36^\circ$ or $\beta = 75^\circ$ (Fig. 2). However, experimentally we find that only a rather broad resonance is obtained at $\beta = 36^\circ$ (or 75° , data not shown) as shown in Fig. 4(C). The origin of this effect lies in the significant amount of dipolar broadening in the KMnO_4 system, and this dipolar broadening is only significantly averaged at $\beta = 54.7^\circ$. Similar results are achieved with the system $\text{Mn}_2(\text{CO})_{10}$, Fig. 4(D), which although it contains a species having a relatively large quadrupole coupling constant ($e^2qQ/h = 3.5$ MHz, $\eta = 0.3$, Ref. 25) and should be a better choice for variable-angle sample-spinning, the presence of a strong metal-metal (Mn-Mn) bond introduces a large dipolar contribution to the linewidth, thereby making VASS experiments less successful. Presumably, very high-field MASS operation (≥ 14 T) would produce optimum resolution for $\text{Mn}_2(\text{CO})_{10}$, since dipolar and CSA terms would be averaged, and the reduced second-order term decreased by ~ 4 by MASS. An experiment carried out at 8.45 T is shown in Fig. 4(D). Alternatively, homonuclear dipolar-decoupling using some type of multiple-pulse scheme could presumably be employed to reduce the strength of the Mn-Mn interaction.

Overall then, the results we have discussed above indicate that variable-angle sample-spinning (VASS) NMR is a promising new technique for high resolution NMR of nonintegral-spin quadrupolar solids. In common with MASS averaging of dipolar interactions, VASS experiments benefit from the fastest spinning speeds possible. In contrast to MASS averaging of CSA interactions, VASS experiments are probably generally best carried out at the very highest magnetic field strengths possible, at least when only quadrupole interactions are of concern and the chemical species of interest have significantly different chemical shifts. In some instances, however, low field operation may yield improved resolution due to a "spreading" effect induced by the second-order quadrupolar frequency shifts.²⁴

The results shown in this paper indicate that VASS is most likely to be of utility in systems which have relatively "dilute" quadrupolar nuclei, e.g., in oxide lat-

tices or aluminosilicates, polyoxometallates, glasses and so on. By combining such high-speed, high-field, variable-angle spinning techniques with both homo and heteronuclear dipolar decoupling techniques, and by development of scaling methods for reduction of second-order interactions, it should thus soon be possible to obtain in a fairly routine manner high-resolution NMR spectra of a large number of interesting quadrupolar nuclei in inorganic solids, thereby opening up new areas of chemical research.

ACKNOWLEDGMENTS

We thank Dr. Akira Naito for useful discussions, and Dr. Michael D. Meadows for his help with probe design and construction.

- ¹E. R. Andrew, Arch. Sci. (Geneva) **12**, 103 (1959).
- ²E. R. Andrew, A. Bradbury, and R. G. Eades, Nature **183**, 1802 (1959).
- ³I. J. Lowe, Phys. Rev. Lett. **2**, 285 (1959).
- ⁴E. R. Andrew, Intl. Rev. Phys. Chem. **1**, 195 (1981).
- ⁵H. Kessemeir and R. E. Norberg, Phys. Rev. **155**, 321 (1967).
- ⁶A. Tzalmona and E. R. Andrew, in Proceedings of the Congress on Magnetic Resonance and Related Phenomenon, Ampere, 18th, 1974, p. 241.
- ⁷R. Eckman, M. Alla, and A. Pines, J. Magn. Res. **41**, 440 (1980).
- ⁸A. Abragam, *The Principles of Nuclear Magnetism* (Clarendon, Oxford, 1961).
- ⁹D. Müller, W. Gessner, H.-J. Behrens, and G. Scheler, Chem. Phys. Lett. **79**, 59 (1981).
- ¹⁰D. Freude and H.-J. Behrens, Cryst. Res. Tech. **16**, K36 (1981).
- ¹¹E. Kundla, A. Samoson, and E. Lippmaa, Chem. Phys. Lett. **83**, 229 (1981).
- ¹²M. D. Meadows, K. A. Smith, R. A. Kinsey, T. M. Rothgeb, R. P. Skarjune, and E. Oldfield, Proc. Natl. Acad. Sci. U.S.A. **79**, 1351 (1982).
- ¹³E. Oldfield, R. A. Kinsey, B. Montez, T. Ray, and K. A. Smith, J. Chem. Soc. Chem. Commun. 254 (1982).
- ¹⁴D. J. Burton and R. K. Harris, J. Chem. Soc. Chem. Commun. 256 (1982).
- ¹⁵E. Oldfield, S. Schramm, M. D. Meadows, K. A. Smith, R. A. Kinsey and J. Ackerman, J. Am. Chem. Soc. **104**, 919 (1982).
- ¹⁶U. Haeberlen, *High Resolution NMR in Solids* (Academic, New York, 1976).
- ¹⁷A. Naito, S. Ganapathy, and C. A. McDowell, J. Mag. Res. (in press).
- ¹⁸H. Goldstein, *Classical Mechanics* (Addison-Wesley, Reading, Mass., 1950).
- ¹⁹J. F. Baugher, P. C. Taylor, T. Oja, and P. J. Bray, J. Chem. Phys. **50**, 4914 (1969).
- ²⁰A. Nolle, Z. Phys. A **280**, 231 (1977).
- ²¹G. F. Lynch and S. L. Segel, Can. J. Phys. **50**, 567 (1972).
- ²²W. Gauss, S. Günther, A. R. Haase, M. Kerber, D. Kessler, J. Kronenbitter, H. Krüger, O. Lutz, A. Nolle, P. Schrade, M. Schüle, and G. E. Sieglösch, Z. Naturforsch., A **33**, 934 (1978).
- ²³H. E. Petch and K. S. Pennington, J. Chem. Phys. **36**, 1216 (1962).
- ²⁴S. Schramm and E. Oldfield, J. Chem. Soc. Chem. Commun. (in press).
- ²⁵E. S. Mooberry, H. W. Spiess, and R. K. Sheline, J. Chem. Phys. **57**, 813 (1972).